Phased array antenna controlled by FPGA-ARM Cortex-M Processor

W. Amara[1], R. Ghayoula [2], A. Hammami[3], A. Smida [4], I. El Gmati[5] and J. Fattahi[6]
[1]SysCom Laboratory, ENIT, University of Tunis El Manar, Tunis 1068, Tunisia
[2]Faculty of engineering, Moncton University, New Brunswick, Canada
[3]Laboratory (IRESCOMATH), ISSIG, University of Gabes, Tunisia
[4]Department of Medical Equipment Technology, College of Applied Medical Sciences, Majmaah University, Almajmaah 11952, KSA
[5]College of Engineering at Al Gunfudha Umm Al Qura University, KSA
[6]Department of Computer Science and Software Engineering at Laval University, Canada
Correspondence: ridha.ghayoula@umoncton.ca (R.G.); iagmati@uqu.edu.sa (I.E.G.)

ABSTRACT This paper discusses the architecture of an adaptive transmitting antenna array that allows highly flexible beamsteering. Antenna arrays are used in many digital signal processing applications due to their ability to locate signal sources. The Direction of Arrival (DOA) estimation is a key task of array signal processing, with the Taguchi method and Multiple Signal Classification (MUSIC). Although various algorithms have been developed for DOA estimation, their high complexity prevents their use in real-time applications. In this paper, we design and develop an implementation using Field Programmable Gate Array (FPGA Artix-7), which is the most widely used ARM processor in embedded systems. The antenna array is digitally controlled with the phases synthesized by the Taguchi method.

INDEX TERMS Phased antenna array, FPGA-Artix-7, MUltiple SIgnal Classification (MUSIC), Taguchi, DOA.

I. INTRODUCTION

Phased array usually means an electronically scanned array, a computer-controlled array of antennas that creates a beam of radio waves that can be electronically steered to point in different directions without moving the antennas [1]- [2]. Determining the phase shift in accordance with the desired direction of beamforming involves complex mathematical calculations and is done by a computer system.Phased array antennas can be electrically steerable, which means the physical antenna can be stationary. This concept can eliminate all the headaches of a gimbal in a radar system. It can keep an antenna locked onto a satellite when mounted on a moving platform.
There are a various of ways to excite array antennas, depending on the arrary's desired characteristics. Generally, transmission lines must be run to each antenna element [3]- [4] .

The amplitude and phase of the element excitations can be varied using discrete amplitude/phase shifting devices, the feed array, or a combination of both. A multi-element phased array can be partitioned into sections, making it suitable for some MIMO applications [5]. For example, the 64-element array could be arranged to provide 8x8-element arrays [6]- [7]- [8]. With beam steering capability, the signal path can be optimized for the best performance [10]- [11]- [12].

In [13], beamforming and direction of arrival (DOA) using the MSR-CORDIC and MUSIC algorithms, respectively. The proposed algorithm is developed using Verilog HDL and implemented using the Xilinx field-programmable gate array (FPGA). In [14] the authors propose a new design of a millimeter-wave (mm-Wave) array antenna package with beam steering characteristics for the fifth generation (5G) mobile applications [15]- [16].

In [18], the authors present a beamforming shaped-beam satellite (SBS) antenna based on a phased array technique and a boosted-beam control. The authors explore the existing technologies and suggests improvements for the development of futuristic Active Phased Array Radars [19]- [20]. FPGA-based T/R Module Controller (TRMC) interfaces with the higher level controller over the Low Voltage Differential Signaling in [21]- [22]. The authors present 512-element integrated optical phased arrays with low-power operation in [23]. In this work, we are interested in the implementing of a phased antenna array control based on Xilinx Artix-7. The phases are synthesized with the Taguchi method according to the angles estimated by the MUSIC algorithm. We will combine these two techniques to have an adaptive system and in real-time [24]- [25] .

The organization of the paper is as follows. In section II, we have developed an antenna array with Signal Model and Estimation Algorithm (MUSIC) and Taguchi's algorithm. Section III presents synthesis results and FPGA design using an ARM processor with Xilinx Vivado 2019.2. Finally, the conclusions of this work are summarized in Section IV.

II. ANTENNA ARRAY

Smart Antennas are phased array antennas with smart signal processing algorithms used to identify the angle of arrival (AOA) of the signal, which can be used subsequently to calculate beam-forming vectors [26].

A. SIGNAL MODEL AND ESTIMATION ALGORITHM (MUSIC)

Characterized by an array of covariance decomposition, the following conclusions can be drawn [27]:
The eigenvalues of the matrix R_x are sorted in accordance with size, which is

$$\lambda_1 \geq \lambda_2 \geq ... \geq \lambda_M > 0, \tag{1}$$

where larger eigenvalues D are correspond to signal while $M - D$ smaller eigenvalues are correspond to noise. The eigenvalues and eigenvectors which belong to matrix R_x are correspond to signal and noise, respectively. Therefore, the eigenvalue of R_x to signal eigenvalue and noise eigenvalue can be divided [27]- [28].

Let the number of signal sources $k(k = 1, 2, \ldots, D)$ to the antenna array, the wavefront signal be $S_k(t)$, as previously assumed, $S_k(t)$ is a narrowband signal, and $S_k(t)$ can be expressed in the following form

$$S_k\left(t\right) = s_k\left(t\right) e^{jwk(t)} \tag{2}$$

where $s_k(t)$ is the complex envelope of $S_k(t)$ and $w_k(t)$ is the angular frequency of $S_k(t)$. As assumed before, all signals have the same center frequency. So

$$w_k = w_0 = \frac{2\pi c}{\lambda} \tag{3}$$

where c is electromagnetic wave velocity, is wave length.

So use the first array element as reference points. At the moment t, the induction signal of the array element $m(m = 1, 2, \ldots M)$ to the k-th signal source in the spaced linear array is

$$a_k s_k\left(t\right) e^{-j(m-1)\frac{2\pi d sin\theta_k}{\lambda}} \tag{4}$$

where a_k is the impact of array element m on the signal source k-th. As assumed before, each array element has no direction, so let $a_k = 1$. Then the output signal of the array element m is

$$x_k(t) = \sum_{k=1}^{D} a_m(\theta_k) s_k(t) + n_m(t) \tag{5}$$

where $s_k(t)$ is the signal strength of signal source k. This expression can be described by matrices:

$$X = AS + N \tag{6}$$

where

$$X = [x_1(t), x_2(t), ..., x_M(t)]^T \tag{7}$$

$$S = [S_1(t), S_2(t), ..., S_D(t)]^T \tag{8}$$

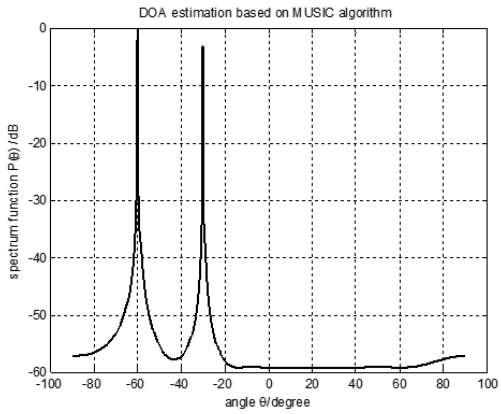

FIGURE 1. MUSIC algorithm -30^o and -60^o

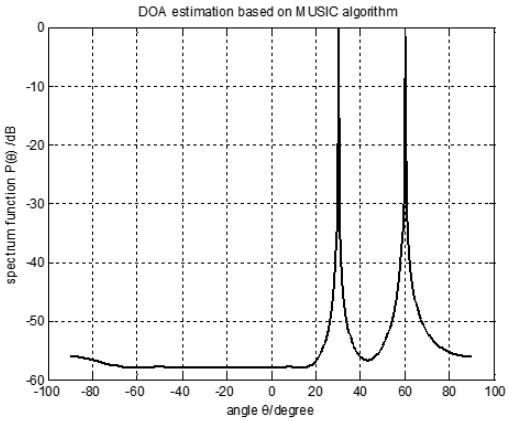

FIGURE 2. MUSIC algorithm 30^o and 60^o

$$A = [a(\theta_1), a(\theta_1), ..., a(\theta_D)]^T \tag{9}$$

$$N = [n_1(t), n_1(t), ..., n_M(t)]^T \tag{10}$$

Let λ_i be the i-th eigenvalues of the matrix R_x, v_i isthe eigenvector corresponding to $lambda_i$, then:

$$R_x v_i = \lambda_i v_i \tag{11}$$

let $\lambda_i = \sigma^2$ be the minimum of R_x.

Using noise characteristic value as each column, construct a noise matrix En can be constructed:

$$E_n = [V_{D+1}, V_{D+2}, ..., V_M] \tag{12}$$

to define spatial spectrum $P_{mu}(\theta)$ can be defined:

$$P_{mu}(\theta) = \frac{1}{a^H(\theta) E_n E_n^H(\theta) a(\theta)} = \frac{1}{\|E_n^H a(\theta)\|^2} \tag{13}$$

Calculate the spectrum function, then obtain the estimated value of DOA by searching the peak.

There are two independent narrowband signals, the incident angle is (-30°, 30°) and (-60°, 60°) respectively; those two signals are not correlated, the noise is ideal Gaussian

white noise, the SNR is 20dB, the element spacing is half of the input signal wavelength, array element number is 8 [28].

B. TAGUCHI PHASE ANTENNA ARRAY SYNTHESIS

The electromagnetic field produced by an antenna array is the vector sum of the fields produced by each of the elements. By suitably choosing the spacing between the elements and the phase of the current flowing in each, we can modify the directivity of the network thanks to constructive interference in some directions and destructive interference in other directions. In the array of transverse emission antennas, the maximum emission lobe is located in an "equatorial" plane because, in this plane and far from the array, each point is located at the same distance from each of the antennas [29]. Consider an array of $(N\ )$ identical elements separated by distance $w_1, w_2, ..., w_{N-1}$ with element pattern $f\,(\theta)$ and spacing between the $(n\ )$ and $(n+1\ )$ element is $w_n$where $n = 1, 2, ..., N$. Assuming no mutual coupling, the radiated field is [10]:

$$E \cong f\,(\theta)\, e^{(-jkR)} AF\,(\theta) \tag{14}$$

Where $AF\,(\theta)$ is the array factor and is equal to:

$$AF\,(\theta) = \sum_{n=1}^{N} V_n^{(0)} exp\left[jk\left(\sum_{i=1}^{N-1} w_i\right)\sin\theta\right] \tag{15}$$

The Array Factor AF for a linear antennas array is described by the following equation

$$AF(\theta) = 2\sum_{n=1}^{4} a(n) cos\left[\beta d(n) cos\theta\right] \tag{16}$$

The objective function (fitness) is chosen according to the optimization objective where one seeks to minimize the difference between the desired and synthesized radiation pattern.

$$Fitness = \int_0^{180^o} \left|AF_d(\theta) - AF(\theta)\right| d\theta \tag{17}$$

All stages of the Taguchi method are detailed in the reference [17].

$$LD_1 = \frac{(\max - \min)}{s+1} \tag{18}$$

where "max" and "min" are the upper and lower bounds of the optimization range, respectively. The fitness value is used to calculate the corresponding S/N ratio (η) in Taguchi's method through the following formula.

$$\eta = -20\log\left(Fitness\right)(dB) \tag{19}$$

.

$$\bar{\eta}\,(m,n) = \frac{1}{N} \sum_{i, OA(i,n)=m} \eta_i \tag{20}$$

$$\varphi_n|_{i+1}^2 = \varphi_n|_i^{opt} \tag{21}$$

For the $(i+1)^{th}$iteration.

$$LD_{i+1} = RR\,(i) \times LD_1 = rr^i \times LD_1 \tag{22}$$

Where
$RR(i) = rr^i$ is called the reduced function.

$$\frac{LD_{i+1}}{LD_1} \leq cv \tag{23}$$

Where
cv is converged value (cv=0.001).
$rr =$ reduced function ($rr = 0.8$)

Table I shows the phases optimized by the Taguchi method (8 elements) in the angles of the following points (-15°, 15°), (-30°, 30°) and (-60°, 60°).

C. SIMULATION RESULTS

In this section we have presented the effectiveness of the synthesis Taguchi method of an antenna array. The use of this optimization method provides quite interesting results and has the advantage of escaping local solutions of deterministic methods, the solutions obtained can be qualified as optimal compared to other solutions. They also make it possible to simultaneously control all the electrical and geometric parameters of the network (power supply and spatial distribution). However, they can have a drawback represented by the machine computation time. Indeed, it turns out to be relatively high compared to deterministic optimization methods. The choice of the cost or fitness function must be made in a judicious way because the latter represents the key parameter of the convergence towards an optimal solution.

To validate the simulation results, the software CST (Computer Simulation Technology) was used Microwave Studio is an electromagnetic simulator based on the finite integration technique (FIT). This digital method provides a spatial arrangement of discretization, applicable to various electromagnetic problems, ranging from the computation of static fields to high frequency applications in the time or frequency domain.

The geometric parameters of the test antenna are shown in the Table II.

We find that the antenna radiation is indeed omnidirectional at the 2 GHz frequency, with a simulated gain greater than 7.28 dBi and a linear polarization of the field [30]- [6]- [31]. Fig.6 shows the 3-dimensional radiation pattern. The gain is expressed in dBi, which means that the gain is related to that of an isotropic antenna. Fig. 7 shows the configuration for the simulation of coupling in the plane E. The distance between two elements $d = 65.5mm$. This is limited by the size of the antenna. When the antennas are well matched, the coupling between two elements is directly given by the transmission coefficient S_{ij}. We find that the coupling decreases as a function of the frequency and the coupling is quite weak in the frequency band ($\leqslant 20dB$). The pattern diversity consists in using antennas having different directions of radiation. At the mobile level, it can be caused by the proximity of the antennas. Indeed, when the antennas

TABLE 1. The phases optimized by the Taguchi method (8 Elements)

Elements#	@-60°	@-30°	@-15°	@15°	@30°	@60°
$\varphi(1)$	174.3682	44.7543	-163.549	162.8153	-45.6766	-174.7232
$\varphi(2)$	-29.9990	134.5562	-116.5289	116.2577	-135.5335	29.4385
$\varphi(3)$	125.9226	-135.3424	-70.1742	69.6776	134.9528	-126.3971
$\varphi(4)$	-77.7991	-45.2283	-23.5098	23.4367	44.7562	77.7486
$\varphi(5)$	77.7991	45.2283	23.5098	-23.4367	-44.7562	-77.7486
$\varphi(6)$	-125.9226	135.3424	70.1742	-69.6776	-134.9528	126.3971
$\varphi(7)$	29.9990	-134.5562	116.5289	-116.2577	135.5335	-29.4385
$\varphi(8)$	-174.3682	-44.7543	163.549	-162.8153	45.6766	174.7232

TABLE 2. Antenna Parameters

Parameters	Description	values (mm)
L	Length of the antenna	41.6
W	Width of the antenna	52.03
L_m	Length of the ligne	25.03
W_m	Width of the ligne	0.58
L_f	Feed ligne	25.03
W_f	Height	1.88
h	Rogers-RO3003	0.762

are close, the inter-element coupling generates a deformation of the radiation patterns. These can then be exploited to obtain diversity with minimum bulk. However, you must be careful because inter-element couplings can lead to a loss of power. In addition, in the case of small angular propagation deviations, there is little or no diversity of the received signal. To validate the operating principle of the proposed system, we simulated the radiation patterns of this antenna array with CST Microwave Studio software [32]- [33].

III. SYNTHESIS RESULTS AND FPGA VERIFICATION

With the storage of the phases already synthesized in the BRAM memory, we can directly access the synthesized weightings without going through mathematical calculations since we have all the possible cases, and to adapt these weightings to the requirements of digital phase shifters we must go through a setting on the scale of the weightings synthesized with the addition of 360° for each negative phase. Then create a virtual image to temporarily store the list of phases having negative positions. Then a quantization (on 8 bits) of all the stored phases using equations (24,25) and (26).

In what follows, we will apply the phase quantification technique.
The algorithm for this technique is as follows:
- Define the phase interval $[\varphi_{min}, \varphi_{max}]$
- Define the number of coding bits nb.
- We calculate the smallest significant bit lsb_φ

$$lsb_\varphi = \frac{\varphi_{max}}{2^{nb-1} - 1} \tag{24}$$

Let φ excitation phase,φ_{ent} the relative integer representation of φ and φ_{quan} the representation quantified of φ.

$$\varphi_{ent} = round\left(\frac{\varphi}{lsb_\varphi}\right) \tag{25}$$

$$\varphi_{quan} = \varphi_{ent} \times lsb_\varphi \tag{26}$$

The evolution of the phase quantization error as a function of the number of coding bits shows that this error decreases with the number of coding bits and when choosing a number of bits of coding equal to 8, the error becomes acceptable. So it is better to use 8 bits for the phase encoding. Finally, a rounding of the values obtained before storing them again in a matrix in the memory, in order to prepare them for the excitation of the digital phase shifters.

The FPGA implementation of the proposed beamforming algorithm is developed as shown in Fig. 3, the same setup will be used to develop the FPGA-ARM beamformer. The proposed beamforming algorithm consumes 7168 LUTs, 8243 flip flops, 29 BRAMs, 3 DSPs and 237 LUTRAM and 61 IOBs as shown in Table III.

TABLE 3. Resource allocation-Artix-7 XC7A35TICSG324-1L

Resources	Utilization	Available	Utilization (%)
LUT	7168	20800	34.46
LUTRAM	237	9600	2.47
FF	8243	41600	19.81
BRAM	29	50	58.00
DSP	3	90	3.33
IO	61	210	29.05
BUFG	4	32	12.50
MMCM	1	5	20.00

IV. CONCLUSION

In this paper we have set up the necessary elements of an electronic scanning antenna using FPGA Artix-7 with an ARM processor. By the realization of this prototype, we have proved the feasibility of this system by using controlled phase shifters (Phase Shifters), an antenna array , an algorithm for the detection of directions of arrival and a beamforming system DOA adaptive in emission / reception using the Taguchi method this system is driven by FPGA Artix-7 control boards.

This complete study made it possible to update a new electronic scanning antenna system, presenting particularly interesting and satisfactory performances although certain points should be improved for example, it would be possible to take into account coupling between the antennas and the integration of all this system in a single card. The results

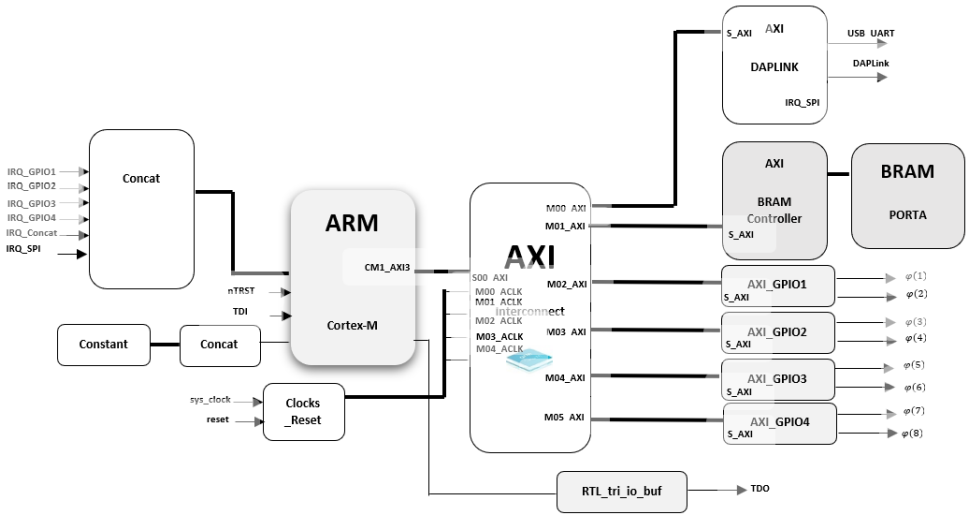

FIGURE 3. Internal control circuit architecture based on ARM processor and Xilinx Artix-7-XC7A35TICSG324-1L

TABLE 4. The address ranges of the design-Artix-7 XC7A35TICSG324-1L

CortexM1	Slave interface	Base Name	Offset Address	Range	High Address
axibram	S_AXI	Mem0	ox6000_0000	8K	ox6000_1FFF
axigpio	S_AXI	Reg	ox4011_0000	64K	ox4011_FFFF
axigpio	S_AXI	Reg	ox4012_0000	64K	ox4012_FFFF
axigpio	S_AXI	Reg	ox4004_0000	64K	ox4004_FFFF
axigpio	S_AXI	Reg	ox4005_0000	64K	ox4005_FFFF

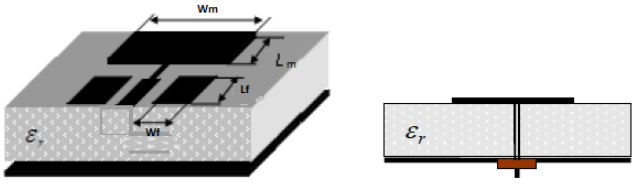

FIGURE 4. Antenna geometry

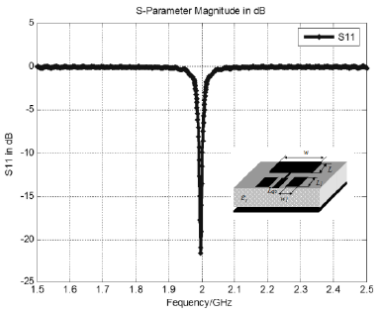

FIGURE 5. S_{11}dB

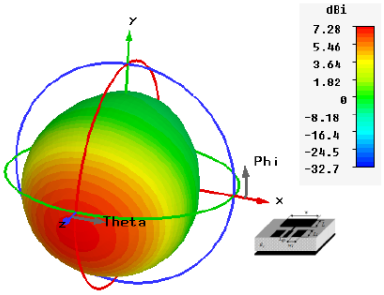

FIGURE 6. Radiation pattern of a patch antenna at f = 2 GHz

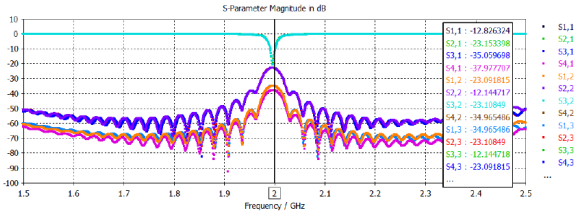

FIGURE 7. Results of the coupling between the elements in the E plane

obtained show the feasibility and efficiency of using the Taguchi method in the synthesis of linear antenna array radiation patterns.

ACKNOWLEDGMENT

The authors would like to thank the Deanship of scientific Research Umm AL-Qura University for supporting this work by Grant code (23UQU4361156DSR02)

ABBREVIATIONS

MUSIC MUltiple SIgnal Classification
DOA Direction Of Arrival
FPGA Field Programmable Gate Array
RAM Random Access Memory

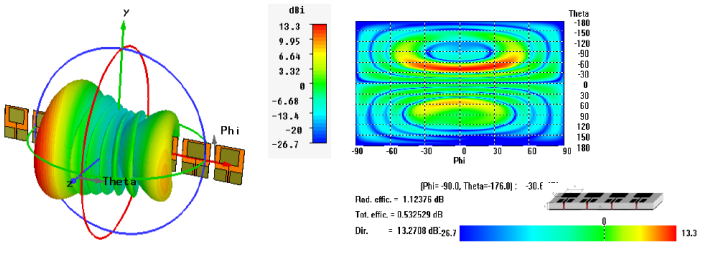

FIGURE 8. Radiation pattern of an antenna array of 8 elements (f = 2 Ghz) @ -60°

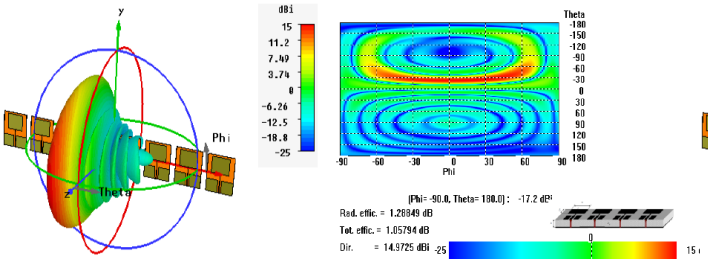

FIGURE 9. Radiation pattern of an antenna array of 8 elements (f = 2 Ghz) @ -30°

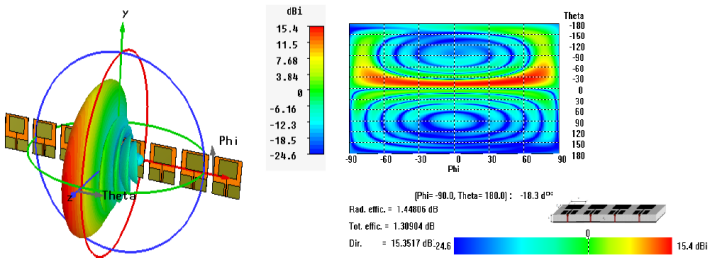

FIGURE 10. Radiation pattern of an antenna array of 8 elements (f = 2 Ghz) @ -15°

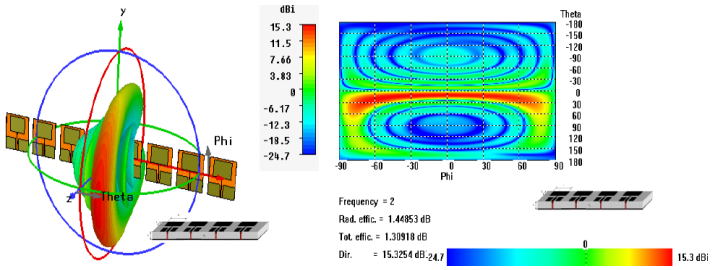

FIGURE 11. Radiation pattern of an antenna array of 8 elements (f = 2 Ghz) @ 15°

VHDL Very High-Speed Integrated Circuit Hardware Description Language
TRMC Transmit/Receive Module Controller
LUT LookUp Table
DSPs Digital Signal Processing Elements
FF Flip-Flop
SBS Shaped Beam Satellite

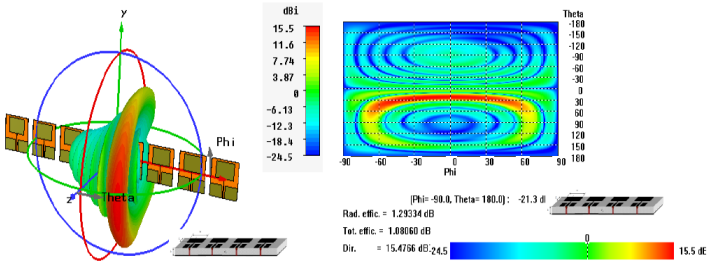

FIGURE 12. Radiation pattern of an antenna array of 4 elements (f = 2 Ghz) @ 30°

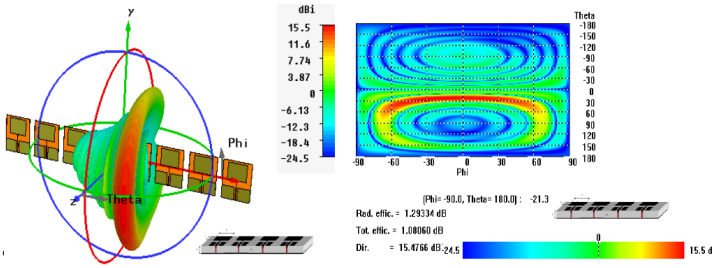

FIGURE 13. Radiation pattern of an antenna array of 8 elements (f = 2 Ghz) @ 60°

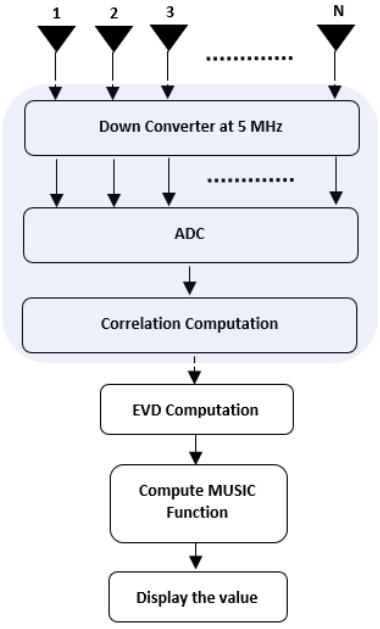

FIGURE 14. Phased Antenna Array (DOA)

REFERENCES

[1] H. Saeidi-Manesh, S. Karimkashi, G. Zhang and R. Doviak, "High-isolation low cross-polarization phased-array antenna for MPAR application," Radio Science, vol. 52, pp. 1544-1557, 2017.
[2] C.K. Ghosh and S.K.Parui,"Reduction of mutual coupling between E-shaped microstrip antennas by using a simple microstrip I-section," Microw. Opt. Technol. Lett. 2013, 55, 2544–2549
[3] D. W. Boeringer and D. H. Werner, "Particle swarm optimization versus genetic algorithms for phased array synthesis," IEEE Trans. Antennas Propag., vol. 52, pp. 771–779, Mar. 2004.
[4] D. W. Boeringer, D. H. Werner and D. W. Machuga, "A simultaneous parameter adaptation scheme for genetic algorithms with application to phased array synthesis," IEEE Trans. Antennas Propag., vol. 53, pp.

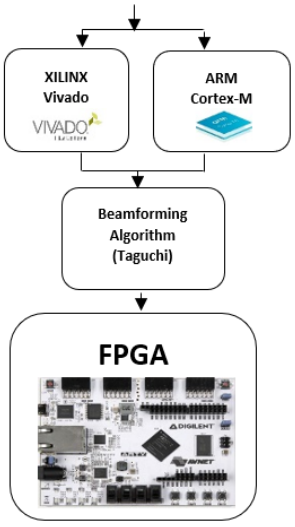

FIGURE 15. Phased Antenna Array (Taguchi control)

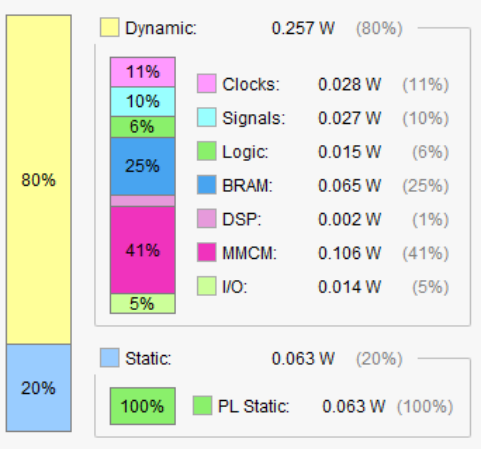

FIGURE 16. Implemented Power Report

356–371, Jan. 2005.

[5] F. Azhiri, R. Abdolee, B. M.Tazehkand, "Effect of mutual coupling on the performance of STCM-MIMO Systems", In IEEE wireless communications and networking conference workshop (WCNCW), 2019.

[6] Z. Li, Z. Du, M. Takahashi, K. Saito and K. Ito, "Reducing Mutual Coupling of MIMO Antennas With Parasitic Elements for Mobile Terminals," IEEE Trans. Antennas Propag, vol. 60, no. 2, pp. 473-481, Feb. 2012.

[7] K. Wei, J.Li, L.Wang, Z. Xing, R. Xu, "S-shaped periodic defected ground structures to reduce microstrip antenna array mutual coupling," Electronics Letters, 52(15), 1288–1290,2016.

[8] N. A. Al-Shalaby, S. G. El-sherbiny, "Mutual coupling reduction of DRA for MIMO applications," Advanced Electromagnetics, 8(1), 1–75, 2019

[9] K. Wei, J.Li , L.Wang, Z. Xing and R.Xu, "S-shaped periodic defected ground structures to reduce microstrip antenna array mutual coupling. Electronics Letters, 52(15), 1288–1290,2016

[10] H. Singh , H. L. Sneha and R. M. Jha, "Mutual Coupling in Phased Arrays: A Review," International Journal of Antennas and Propagation,2013

[11] H. Bilel, L.Selma and A.Taoufik ,"Artificial neural network (ANN) approach for synthesis and optimization of (3D) three-dimensional periodic phased array antenna," . In 2016 17th IEEE International Symposium on Antenna Technology and Applied Electromagnetics (ANTEM-Montreal, Canada) July, (pp. 1-6), 2016

[12] X. Chen, M. Abdullah, Q. Li, J. Li, A. Zhang and T. Svensson, "Characterizations of mutual coupling effects on switch-based phased array antennas for 5G millimeter-wave mobile communications," IEEE Access, vol. 7, pp.31376-31384, 2019.

[13] C.Thiripurasundaria, V.Sumathyb and C.Thiruvengadamc, "An FPGA implementation of novel smart antenna algorithm in tracking systems for smart cities," Computers Electrical Engineering, Volume 65, pp 59-66, January 2018

[14] N.Ojaroudiparchin, M.Shen, S.Zhang and G.F. Pedersen, "A Switchable 3-D-Coverage-Phased Array Antenna Package for 5G Mobile Terminals," IEEE Antennas and Wireless Propagation Letters, Vol. 15, 2016, pp 1747-1750, 2016

[15] H. Attia, "Highly reduced mutual coupling between wideband patch antenna array using multiresonance EBG structure and defective ground surface," Microwave and Optical Technology, September, 1– 10. https://doi.org/10.1002/mop.32193

[16] F.Benykhlef, "EBG Structures for Reduction of Mutual Coupling in Patch Antennas Arrays," Journal of Communication Software and Systems, 13(1), 9–14.

[17] W-C.Weng, F.Yang and A- Z. Elsherbeni, "Linear Antenna Array Synthesis Using Taguchi's Method: A Novel Optimization Technique in Electromagnetics," IEEE Transactions on Antennas and Propagation, Vol.55, 2007.

[18] S-Mo Moon; S. Yun; In-B. Yom; H.L.Lee, "Phased Array Shaped-Beam Satellite Antenna With Boosted-Beam Control," IEEE Transactions on Antennas and Propagation, Vol. 67, Issue: 12, 2019, Pages 7633-7636, 2019.

[19] M. Kiani-Kharaji, H. Hassani and S. Mohammad-Ali-Nezhad, "Widescan phased array patch antenna with mutual coupling reduction," IET Microwaves, Antennas Propagation, vol. 12, pp. 1932-1938, 2018.

[20] S. Benny and S. Sahoo, "Enhancement in Dual Polarization Phased ArrayAntenna Performance and Calibration Techniques for Weather Radar Ap-plications," 2020 International Symposium On Antennas and Propagation(APSYM), pp. 25-28, 2020.

[21] S. Rathod, A. Raut, A. Goel, K. Sreenivasulu, K.S.Beenamole and K.P. Ray,"Novel FPGA based T/R Module Controller for Active Phased Array Radar," 2019 IEEE International Symposium on Phased Array System Technology (PAST),Waltham, MA, USA, 2019.

[22] S. Rathod, K.Sreenivasulu, K.S. Beenamole and K.P.Ray, "Evolutionary Trends in Transmit/Receive Module for Active Phased Array Radars", Defence Science Journal, Vol. 68, No. 6, 2018, pp 553-559, 2018.

[23] C. V. Poulton, M. J. Byrd, E. Timurdogan, P. Russo, D. Vermeulen and M. R. Watts, "Optical Phased Arrays for Integrated Beam Steering," 2018 IEEE 15th International Conference on Group IV Photonics (GFP), pp 1-2, 2018.

[24] D.K. Ntaikos and T.V. Yioultsis, "Compact split-ring resonator-loaded multiple-input–multiple-output antenna with electrically small elements and reduced mutual coupling," IET Microw Antennas Propag., pp 421–429, 2013.

[25] F. Liu, J. Guo and L. Zhao ,"Ceramic superstrate-based decoupling method for two closely packed antennas with cross-polarization suppression," IEEE Trans Antennas Propag. 2020, 69(3), 1751–1756, 2020.

[26] A. H. Naqvi and S.Lim ,"Review of recent phased arrays for millimeter-wave wireless communication, " MDPI Sensors 2018, 18(10), 3194, May 2021.

[27] Z. Wang, W. Xie and Q.Wan, "SCC-MUSIC algorithm for DOA estimation based on cyclostationarity," CIE International Conference on Radar (RADAR),Guangzhou, China, 2016

[28] E. Ghayoula, J. Fattahi, R. Ghayoula, E. Pricop, G. Stamatescu, J.-Y. Chouinard and A. Bouallegue,"Sidelobe level reduction in linear array pattern synthesis using Taylor-MUSIC algorithm for reliable IEEE 802.11 MIMO applications, " IEEE International Conference on Systems, Man, and Cybernetics (SMC), Budapest, Hungary 2016.

[29] M. M. Khodier and C. G. Christodoulou, "Linear array geometry synthesis with minimum sidelobe level and null control using particle swarm optimization," IEEE Trans. Antennas Propag., vol. 53, pp. 2674–2679, Aug. 2005.

[30] S. Abbasiniazare, K. Forooraghi, A. Torabi, and O. Manoochehri, "Mutual coupling compensation for a 1×2 short helical antenna array using split-ring resonators," Electromagnetics, vol. 33, pp. 1-9, 2013.

[31] A. Farahbakhsh, G. Moradi, and S. Mohanna, "Reduction of mutual coupling in microstrip array antenna using polygonal defected ground structure," ACES JOURNAL, vol. 26, pp. 334-339, 2011

[32] B. Hamdi, T.Aguili, H. Baudrand, "Floquet modal analysis to modelize and study 2-D planar almost periodic structures in finite and infinite extent

with coupled motifs," . Progress In Electromagnetics Research B, 62, 63-86, 2015.

[33] H. Bilel and A. Taoufik, "Floquet Spectral Almost-Periodic Modulation of Massive Finite and Infinite Strongly Coupled Arrays: Dense-Massive-MIMO, Intelligent-Surfaces, 5G, and 6G Applications," Electronics 2022, 11(1), 36, 2022.